

# Surface Engineering for MEMS Reliability

ESS5855 Lecture  
Fall 2010

Surface Engineering and  
Microtribology for MEMS<sup>01</sup>

K. Komvopoulos, U.C. Berkeley  
Wear, 1996

# Adhesion and Friction Forces in MEMS: Mechanisms, Measurement, Surface Modification Techniques, and Adhesion Theory<sup>03</sup>

K. Komvopoulos, U.C. Berkeley  
J. Adhesion Sci. Technol., 2003

**Tribology** is the science and technology of interacting **surfaces** in relative **motion**. It includes the study and application of the principles of **friction**, **lubrication** and **wear**.

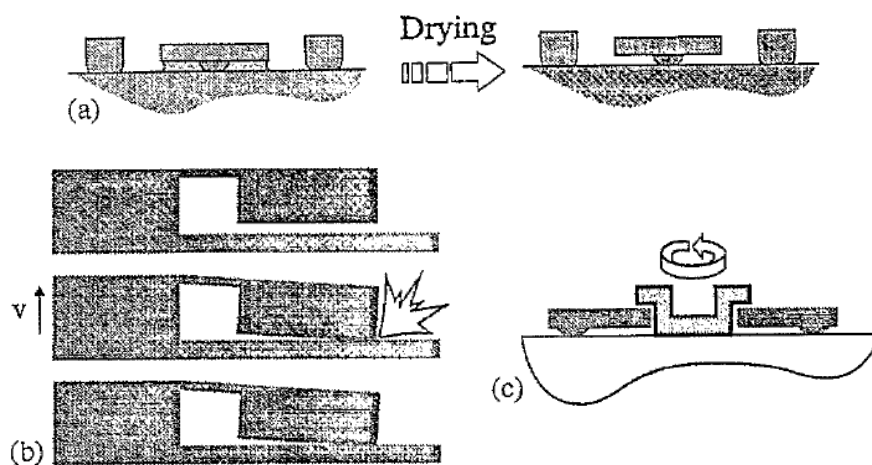


Fig. 3. Typical tribological problems in MEMS: (a) micromachine stiction during release-etch processing, (b) stiction between overdriven suspended mass accelerometer and limit stop, and (c) cross-sectional schematic of electrostatic micromotor showing small-clearance interfaces where intermittent contact may cause wear.

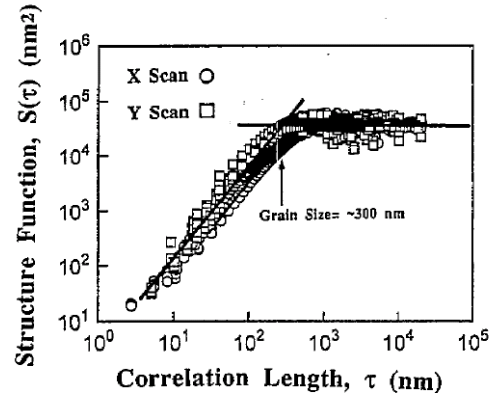
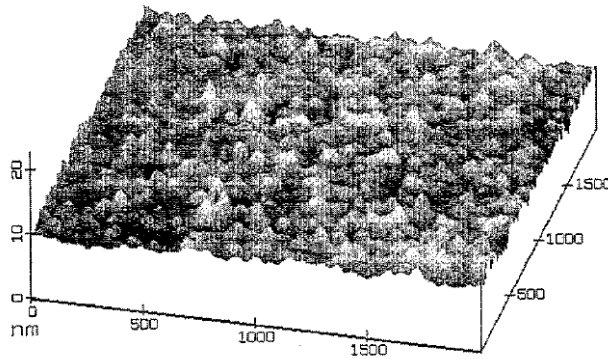
# Abstract

Micromachines, particularly surface micromachines, often include smooth and chemically active surfaces. Because the kinetic energies, start-up forces and torques involved in their operation, and hence available to overcome retarding forces, are necessarily small, surface effects will be critical whenever micromachine contact occurs, whether unintentionally or as part of normal operation. Consequently, basic knowledge of the surface topography characteristics and microscale tribological phenomena arising at micromachine interfaces is of paramount importance to the reliability and robustness of microelectromechanical systems (MEMS). In view of the very small masses and tight tolerances, smooth surfaces, and light loads, characterization of chemomechanical surface interactions must be performed at the microscale. Microtribology is an emerging field dealing with friction and wear phenomena occurring at micrometer scales. Recent developments in this field have begun to lend valuable insight into surface interaction and material property characterization on scales relevant to MEMS. In this publication, the emphasis is on the analysis of various surface micromechanisms, such as solid bridging, liquid meniscus formation, van der Waals force, and electrostatic charging, and the significance of surface roughness and material properties. Experimental and theoretical results for the stiffness of silicon micromachines needed to overcome stiction are compared for different surface roughnesses. The fabrication, basic operation features, and measuring capabilities of microstructures designed specifically to perform microscale tribotesting under controlled conditions are presented. The efficacy of different surface engineering techniques, such as formation of standoff bumps on one of the countersurfaces, roughening (texturing), and surface chemistry modification (e.g. self-assembled monolayers), to reduce high adhesion forces at MEMS interfaces is interpreted in light of analytical and experimental results. It is demonstrated that surface engineering and modification of physicochemical surface properties are effective means of enhancing the reliability and performance of microsystems.

## Outline

- ...
- Surface characterization
- Analysis of surface forces and stiction mechanisms
  - Solid bridging
  - Capillary force
  - Van der Waals force
  - Electrostatic force
  - Asperity deformation force
  - Micromachine critical stiffness
- Friction and wear testing
- Surface modification methods
  - Microstructure deflection
  - Surface topography modification
  - Surface treatments and coating deposition
  - Lubrication by self-assembled monolayers
- ...

# Surface Characterization



# Surface Characterization

$$z(x) = L \left( \frac{G}{L} \right)^{D-1} \sum_{n=0}^{\infty} \frac{\cos \left( 2\pi \gamma^n \frac{x}{L} \right)}{\gamma^{(2-D)n}}$$

$$S(\omega) = \frac{G^{2(D-1)}}{2 \ln \gamma} \omega^{-(5-2D)}$$

$$S_x(\tau) = \langle [z(x+\tau, y) - z(x, y)]^2 \rangle$$

$$\sigma^2 = \int_{-\infty}^{+\infty} \varphi(z) [z - \bar{z}]^2 dz$$

$$S = \frac{1}{\sigma^3} \int_{-\infty}^{+\infty} \varphi(z) [z - \bar{z}]^3 dz$$

$$K = \frac{1}{\sigma^4} \int_{-\infty}^{+\infty} \varphi(z) [z - \bar{z}]^4 dz$$

# Critical Review: Adhesion in Surface Micromechanical Structures<sup>02</sup>

R. Maboudiana's Group, U.C. Berkeley  
J. of Vacuum Sci. and Technol. B, 1997

## Abstract

We present a review on the state of knowledge of surface phenomena behind adhesion in surface micromechanical structures. After introducing the problem of release-related and in-use adhesion, a theoretical frame-work for understanding the various surface forces that cause strong adhesion of micromechanical structures is presented. Various approaches are described for reducing the work of adhesion. These include surface roughening and chemical modification of polycrystalline silicon surfaces. The constraints that fabrication processes such as release, drying, assembly, and pack-aging place on surface treatments are described in general. Finally, we briefly outline some of the important scientific and technological issues in adhesion and friction phenomena in micromechanical structures that remain to be clarified.

# Introduction

- Surface micromachining
  - the fabrication of micromechanical structures from deposited thin films
- The **large surface area** and **small offset from adjacent surfaces** makes microstructures especially vulnerable to adhesion upon contact

## Stiction: Permanent Adhesion

- The **pull-off** force of a displaced surface microstructure in contact with an adjacent surface ranges from a few  **$10^{-6}\text{N}$**  for an airbag accelerometer sense element to **nN** for highly compliant microstructures with submicron flexure widths
- These forces are considerably **weaker** than interfacial forces

# Stiction

- Can occur either
  - during the final steps of the micro-machining process (**release-related adhesion**) or
  - after packaging of the device, due to over-range input signals or electromechanical instability (**in-use adhesion**)

## Theoretical Background

- The causes of strong adhesion can be traced to the interfacial forces existing at the dimensions of microstructures
- **Capillary** force
- **Electrostatic** force
- **van der Waals** force
- **Chemical** force

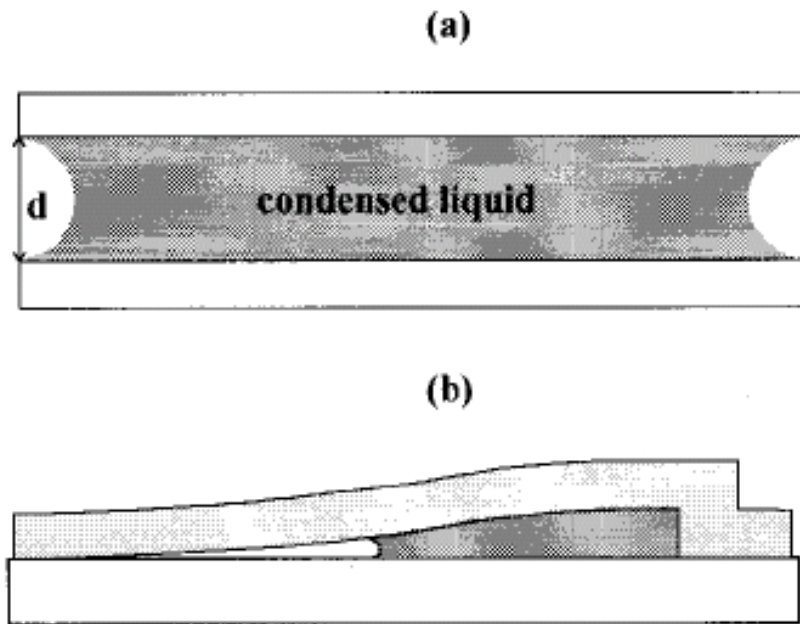


FIG. 2. Schematic diagram of (a) the capillary condensation phenomenon and (b) the microstructure drying process that leads to the adhesion of microstructures to adjacent surfaces.

## Capillary Force

- After the releasing etch is complete, the structure is **rinsed** in de-ionized water to remove the etchant and the etch products
- Either during this phase or upon exposure to air, a layer of **oxide** is formed on the surface of silicon, with **hydroxyl groups** residing on the surface and in the oxide film
- The oxide layer is typically **5~30 Å** thick and has a **high surface energy** due to hydroxyl groups



# Capillary Force

- This surface is **extremely hydrophilic**, and a strong capillary force develops as **the microstructures are pulled out of water** or as **two oxidized silicon surfaces approach one another in a humid environment**
- As a substance crosses the boundary from liquid to gas, the size of the liquid **decreases**
- As this happens, **surface tension** at the solid-liquid interface **pulls** against any structures that the liquid is attached to

## Case 1

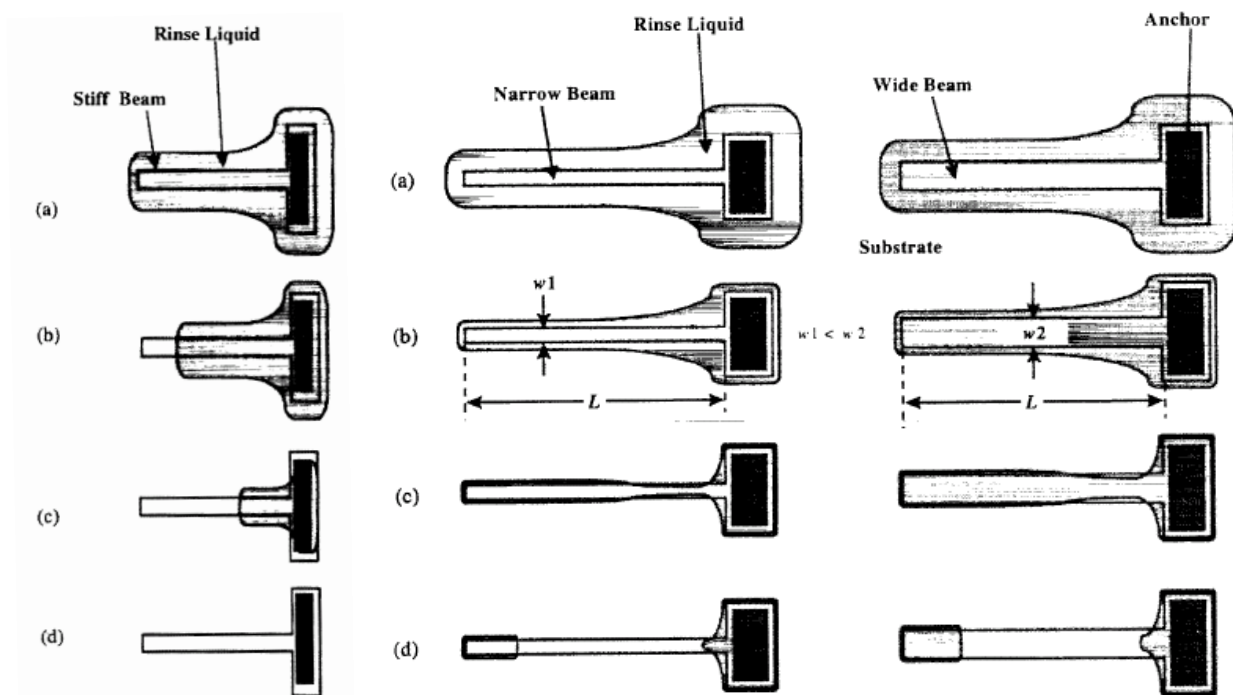
- Consider the situation where the microstructures are **pulled out of water**

$$P_L = \gamma_\ell \left( \frac{1}{r_1} + \frac{1}{r_2} \right) \quad P_L = \frac{2\gamma_\ell \cos \theta}{d}$$

- Drying techniques
  - Freeze sublimation
  - Supercritical carbon dioxide drying

# Comparative Evaluation of Drying Techniques for Surface Micromachining<sup>04</sup>

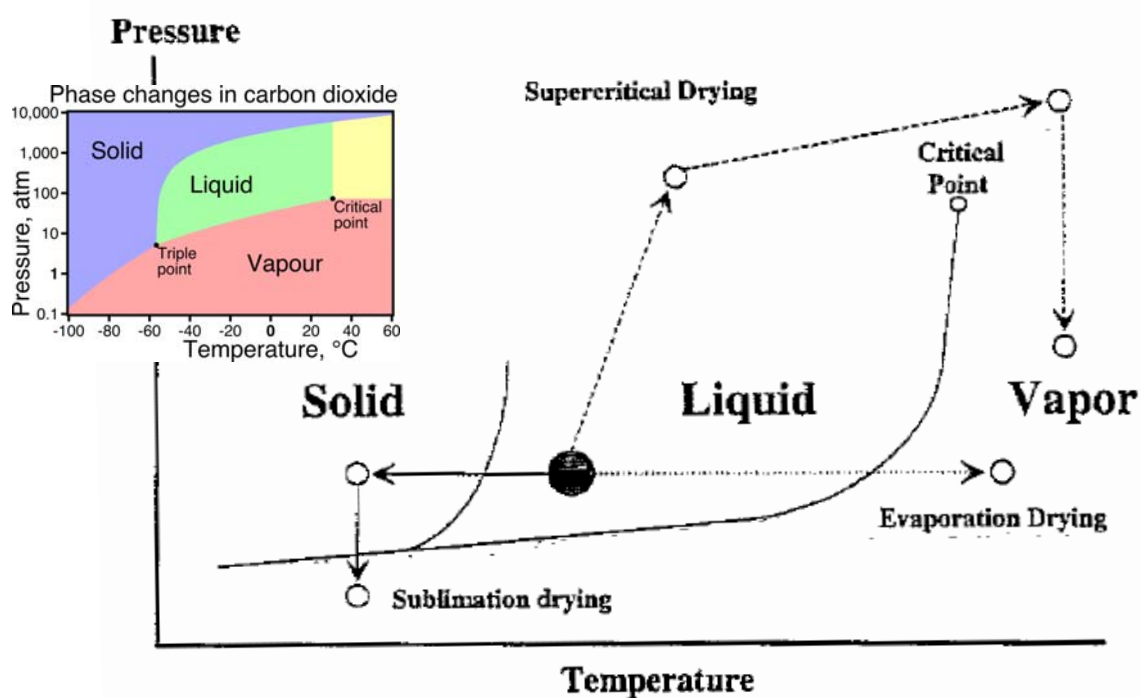
C.J. Kim's Group, UCLA  
Sensors & Actuators A, 1998



# Drying Techniques

- Evaporation drying
  - of DI water
  - with methanol
- Sublimation drying with
  - t-butyl alcohol
  - p-dichlorobenzene
- Supercritical drying with CO<sub>2</sub>

## P-T Graph for Drying Procedures



# Supercritical Drying

- A **critical point** specifies the conditions (temperature, pressure) at which **the liquid state of the matter ceases to exist**
- As a liquid is heated, its density decreases while the pressure and density of the vapor being formed increases
- The liquid and vapor densities become closer and closer to each other until the critical temperature is reached where **the two densities are equal and the liquid-gas line or phase boundary disappears**

Summary of release methods

Release methods	Evaporation drying		Sublimation drying		Supercritical drying
Procedures	HF → DI water	HF → DI water → methanol	HF → DI water → methanol → <i>t</i> -butyl alcohol	HF → DI water → methanol → <i>p</i> -dichlorobenzene	HF → DI water → methanol → carbon dioxide
Melting temp. (°C)	0	−97.5	26	56	−56.4
Boiling temp. (°C)	100	64.7	82.2	173	−78.3
Vapor pressure (torr)	17.54 @20°C 355.3 @80°C	140 @27°C	27 @20°C	1.03 @25°C 10 @54.8°C	N/A
Surface tension (mN m <sup>−1</sup> )	72.88 @25	22.65	20.17	N/A	1.16
<u>Advantages</u>	simple	lower surface tension than DI water	fast sublimation	only hot plate needed	clean excellent results
<u>Disadvantages</u>	mediocre results	mediocre results	requires refrigeration and vacuum absorbs water vapor	toxic needs vacuum contracts upon solidifying	complicated setup

## Case 2

- When two **hydrophilic** surfaces approach each other in a **humid environment**
- Liquids that wet or have small contact angles,  $\theta$ , on surfaces condense from vapor into small cracks and pores in a phenomenon known as **capillary condensation**
- At equilibrium, the meniscus curvature is related to the relative vapor pressure ( $P/P_{\text{sat}}$ ) by the **Kelvin equation**

## Case 2

- Kelvin equation

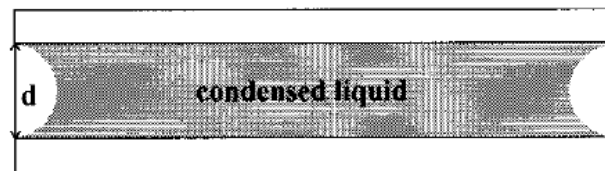
$$\left( \frac{1}{r_1} + \frac{1}{r_2} \right)^{-1} \equiv r_k = \frac{\gamma_l v}{RT \log(P/P_{\text{sat}})}$$

where  $r_1$  and  $r_2$  are the two radii of curvature of the meniscus,  $r_k$  is the Kelvin radius,  $\gamma_l$  is the surface tension of the liquid, and  $v$  is its molar volume ( $\gamma_l v/RT = 0.54 \text{ nm}$  for water at  $20^\circ\text{C}$ )

## Case 2

- For a spherically concave water meniscus, putting  $r_1=r_2=r$ , we find that  $r=\infty$  at  $P/P_{\text{sat}}=1$ , and  $r=-1.6$  nm at  $P/P_{\text{sat}}=0.5$  (50% relative humidity)
- The liquid undergoes capillary condensation as soon as the separation equals

$$d_{0,\text{cap}} = 2r_1 \cos \theta \approx 2r_k \cos \theta.$$



## Case 2

- The effect of a liquid condensate on the adhesion force per unit area between two parallel plates

$$\mathcal{F}_{\text{cap}}(d) = \frac{2\gamma_\ell \cos \theta}{d^2} \left( \frac{V}{A} \right) = \frac{2\gamma_\ell d_{0,\text{cap}} \cos \theta}{d^2}.$$

- As the two surfaces are pulled apart, the meniscus breaks at a separation much larger than  $d_{0,\text{cap}}$
- Integrating from  $d_{0,\text{cap}}$  to infinity yields the work of adhesion

$$\mathcal{W}_{\text{cap}} = 2\gamma_\ell \cos \theta,$$

# Surface Forces & Stiction Mechanisms

- Solid bridging
- Capillary force
- Van der Waals force
- Electrostatic force
- Asperity deformation force
- Micromachine critical stiffness

Fig. 9. Variations of capillary, van der Waals, and electrostatic forces per unit area with the surface separation distance for smooth surfaces [29].

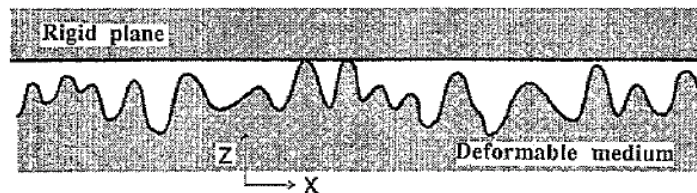
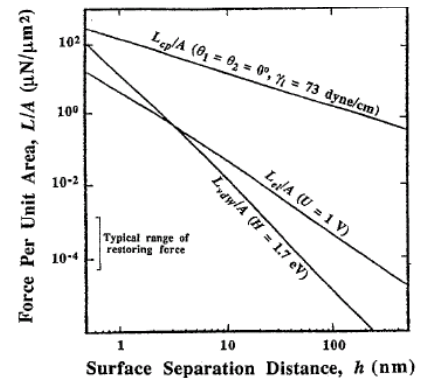


Fig. 8. Equivalent contact model of two rough surfaces.

## Electrostatic Force

- Electrostatic attraction may arise due to electrostatic charging
- Charges are known to accumulate from the ambient and migrate across insulating surfaces on silicon chips
- Can be solved by thickening the oxide and nitride insulating layers to minimize the effect of the surface charge on the underlying silicon device layers

$$\mathcal{F}_{el}(d) = \frac{\epsilon_0 V^2}{2d^2}$$

# van der Waals Force

- For two flat parallel surfaces, and for separations less than a characteristic distance,  $z_0=20$  nm (non-retarded regime), the attractive force per unit area is

$$\mathcal{F}_{\text{vdW}}(d) = \frac{\mathcal{A}}{6\pi d^3}$$

- Taking retardation into account, it is proposed that

$$\mathcal{F}_{\text{vdW}}(d) = \frac{\mathcal{A}}{6\pi} \frac{z_0}{d^3(d+z_0)}.$$

## Solid Bridging

- The formation of **covalent bonds** between two surfaces may also play a role in certain instances
- Observed in cases when the structures are **left to dry** following the final water rinse during the release process
- **Nonvolatile impurities** present in the drying liquid are deposited on the solid surfaces
- Deposition is pronounced in narrow spaces and between contacting surfaces, **cementing** the structures together



# Hydrogen Bonding

- Hydrophilic silicon surfaces contain a large number of hydroxyl groups
- -OH groups can form strong hydrogen bonds as the separation between surfaces becomes small
- The density of hydrogen-bonding sites is given by the number of silanol groups and is found to be about **5 per nm<sup>2</sup>** for a fully hydrated silica surface
- The strength of most hydrogen bonds lies between 10 and 40 kJ/mol, yielding adhesion energies in the range **90~350 mJ/m<sup>2</sup>**

## Implications

- **Capillary forces** dominate

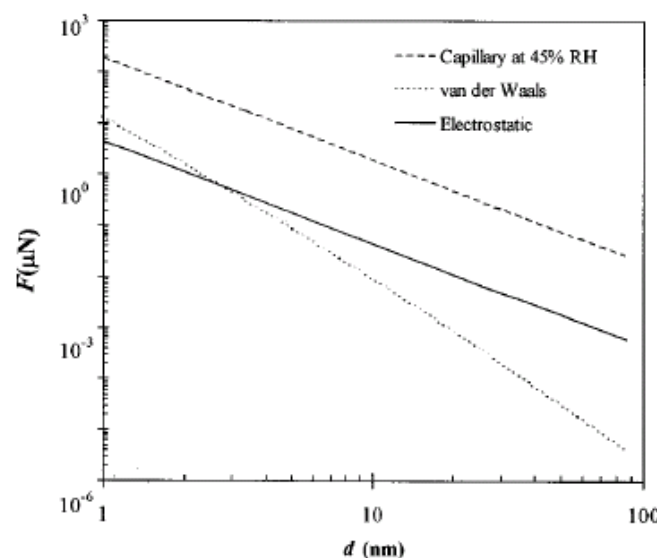


FIG. 3. Comparison of **attractive forces per 1  $\mu\text{m}^2$  area** existing at the dimensions of microstructures as a function of the separation between two perfectly smooth surfaces of silicon.

# Implications

- An effective treatment for these micro-structures must provide a **hydrophobic** surface in order to avoid the formation of **water layers** on the surface, thereby eliminating capillary forces altogether
- The removal of the hydrophilic **hydroxyl groups** from the surface will also eliminate the possibility for hydrogen bonding as the two surfaces come into contact
- To minimize electrostatic attraction, the two surfaces should be **conductive**, allowing charge dissipation to occur effectively
- A reduction in the **effective contact area** is necessary to further reduce the overall adhesion forces in micro-devices

## Mechanical Stability and Adhesion of Microstructures under Capillary Forces<sup>05</sup>

C.H. Mastrangelo and C.H. Hsu, Ford  
J. of MEMS, 1993

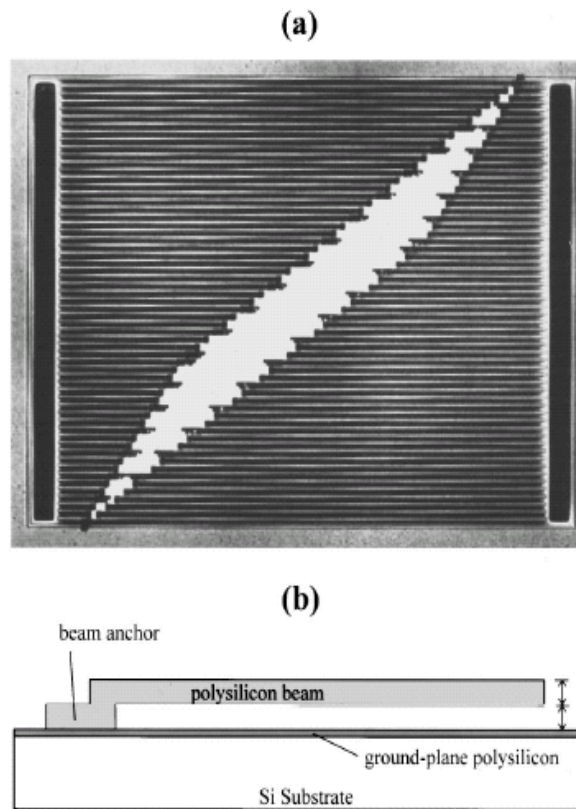


FIG. 4. Cantilever beam array: (a) an optical image; (b) a side-view schematic diagram.

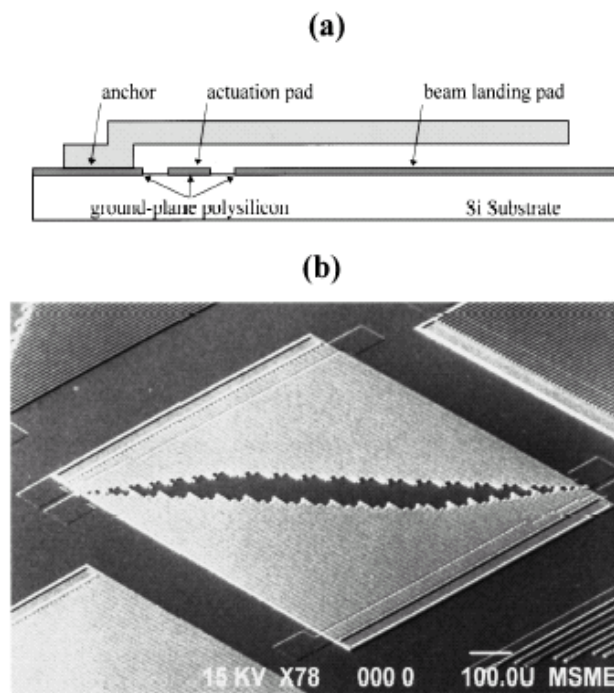


FIG. 5. Electrostatically actuated cantilever beam array: (a) a side-view schematic diagram; (b) a SEM image. In the design of Ref. 45, the beams were about  $10\text{ }\mu\text{m}$  wide,  $2.2\text{ }\mu\text{m}$  thick,  $2\text{ }\mu\text{m}$  off the surface, and their lengths varied from  $50$  to  $260\text{ }\mu\text{m}$  in  $10\text{ }\mu\text{m}$  increments, and then from  $260$  to  $1000\text{ }\mu\text{m}$  in  $20\text{ }\mu\text{m}$  increments.

# Cantilever Beam Array

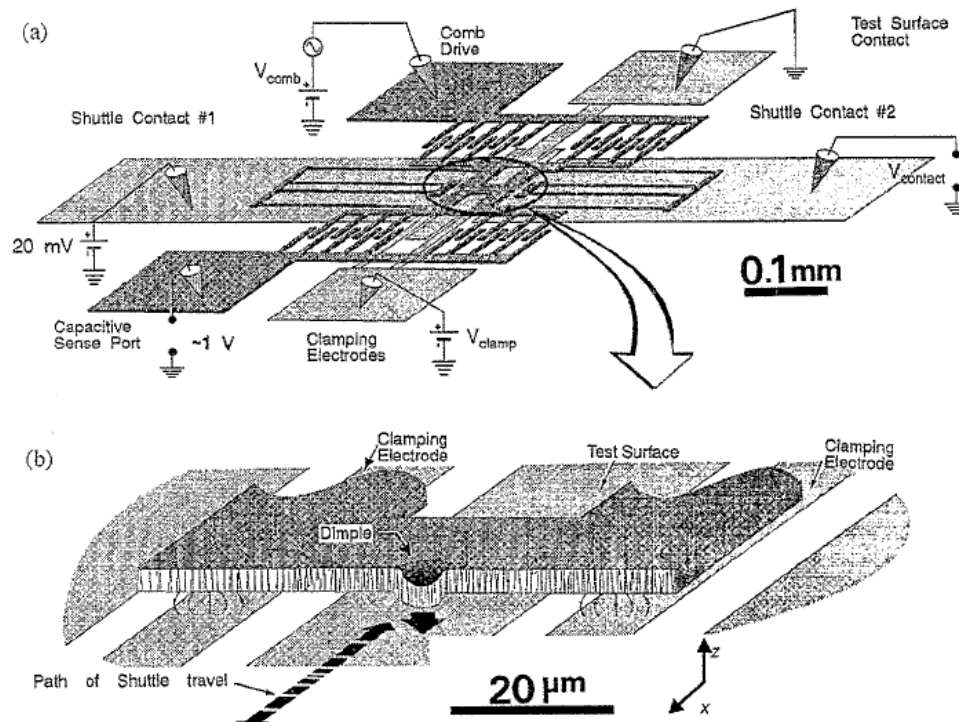
- The **work of adhesion** between surfaces
  - The energy needed to separate unit areas of two adhering surfaces
- The beams are brought into contact with the underlying substrate
- For beams shorter than a **characteristic length**, their stiffness will be sufficient to free them completely from the other surface
- Beams longer than this characteristic length will remain adhered to the surface

# Cantilever Beam Array

- The value of the **detachment length** ( $l_d$ ) is measured as the length at which the beams exhibit a transition from adhered to free standing
- By balancing the **elastic energy** stored within the beam and the beam-substrate interfacial energy, the work of adhesion,  $W$ , between the two surfaces can be calculated

$$W = \frac{3}{8} \frac{Eh^2t^3}{l_d^4},$$

# Friction and Wear Testing



## Topographic Modification of Surfaces

- Reducing post-release adhesion by intentionally **roughening** (texturing) one of the contacting surfaces

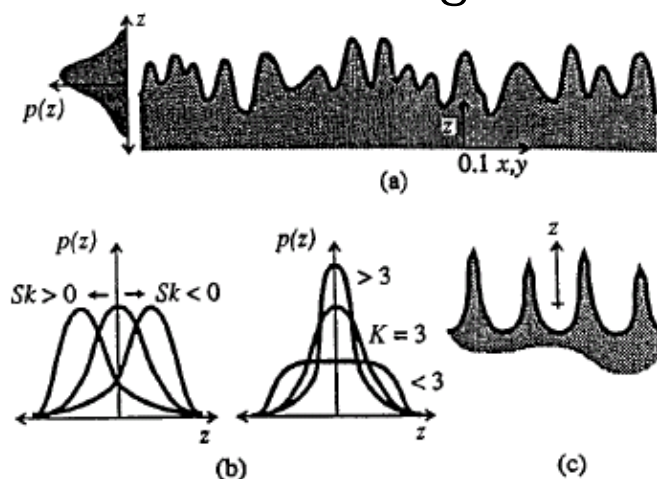


FIG. 7. (a) Structure height distribution function,  $p(z)$ ; (b) significance of reduced skewness,  $Sk$ , and kurtosis,  $K$ , to the shape of  $p(z)$ ; (c) a low-adhesion textured surface.

# Chemical Modification of Surfaces

- Etching away the surface **oxide** and terminating the surface with **hydrogen**
- Coating the surface with thin, organic **self-assembled monolayers**
- Coating the surface with **fluorocarbon** films formed by **plasma polymerization**
- Employing **diamond** and **diamond-like carbon coatings** for reducing adhesion in micro-devices

## Self-Assembled Monolayers

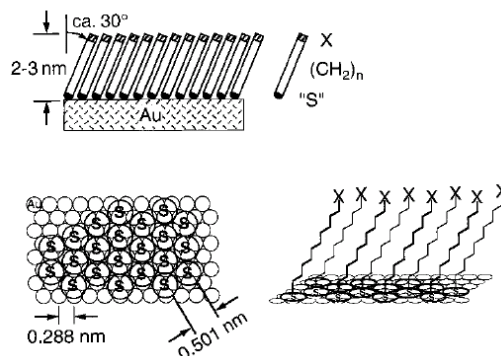
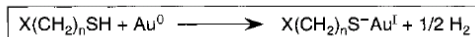
- The most extensively studied SAM coatings deposited on silicon are **octadecyltri-chlorosilane (OTS)** precursor molecules having a chemical formula of  $\text{C}_{18}\text{H}_{37}\text{SiCl}_3$
- When the precursor molecules are placed into a **suitable solvent** such as a 4:1 hexadecane : carbon tetrachloride ( $\text{CCl}_4$ ) mixture and an **oxidized silicon surface** is inserted, the trichlorosilyl head groups hydrolyze and chemisorb to the surface, forming Si-O-Si links to the surface

# Self-Assembled Monolayers

- After formation, the film is further stabilized by **crosslinking** between chains, a process often aided by a **low temperature (100 °C) anneal** after film formation
- When prepared correctly, a SAM-coated Si(100) oxide surface exhibits a water contact angle of **110°**, which corresponds to a surface energy of about 20 mJ/m<sup>2</sup>

# Self-Assembled Monolayers

- The film thickness is about **25 Å**, and the film density is approximately **5 chains per nm<sup>2</sup>** (90% of the density of crystalline polyethylene), indicative of a true monolayer coverage





# Self-Assembled Monolayers

- Storage times of up to **18 months in air** produced indistinguishable thicknesses and contact angles from freshly prepared films
- **Impervious** to hot organic solvents, acidic media, and boiling water
- **Advantages:** long-term stability, low surface-energy, hydrophobic, and densely packed structure

## Thermal Stability of SAM

- Adequate for some packaging processes

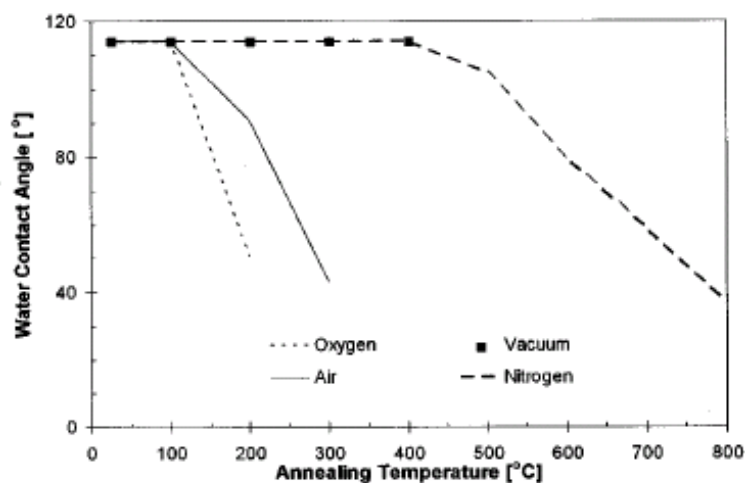


FIG. 18. Water contact angle vs annealing temperature for SAM-coated polysilicon surface under different ambients.



# Implications of SAM Coatings

- The **chlorine** in the OTS precursor molecule is of **corrosion** concern due to the presence of **aluminum** metal interconnect lines
- The ability of these coatings to **survive** in applications involving surfaces **impacting** one another at high speeds need to be studied
- Given that these mono-layers are **insulating** films, the potential problem with **electrostatic charging** must be also examined

## Tribological Challenges in Micromechanical Systems<sup>06</sup>

R. Maboudiana's Group, U.C. Berkeley  
Tribology Letters, 2002

# Reproducibility

- The large number of process variables will make wet chemical processing susceptible to operator errors in many of its critical steps
- More recent coating technologies, which require fewer processing steps, are found to lead to more consistent results across laboratories and operators
- Process automation and sensing for real time monitoring are highly desired
- A novel dry process designed to eliminate many of the steps required by any wet-chemistry based process would be of great interest

# Scale-up

- Scaling up the process from single dies to whole wafers and eventually multi-wafer cassettes
- Proper displacement of solvents from one stage to the next without allowing the wafer to dry and without excessive use of solvents and the associated production of chemical waste

# Wear

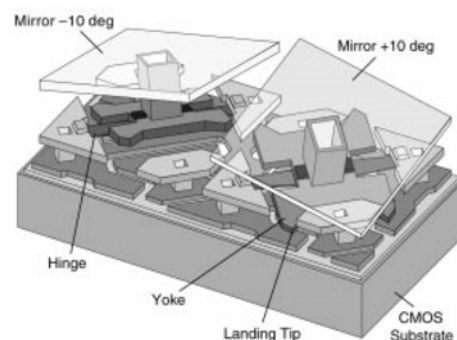
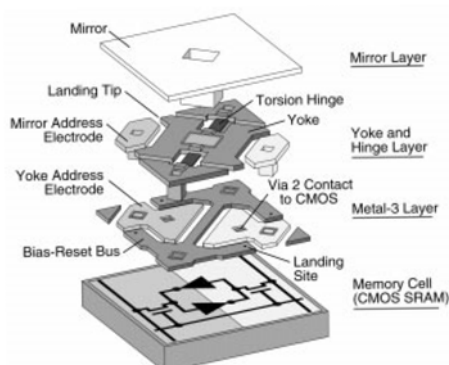
- SAM coatings have been shown to **wear off** when operated under high contact pressure (MPa and higher)
- The SAMs are **thin** (typically a few nm) and can be worn away
- In an **encapsulated** device, one would try to introduce an **excess** of SAM precursor molecules, to create an equilibrium between gas phase and adsorbed phase with **near monolayer equilibrium coverage**

## Lubrication of digital micromirror devices<sup>TM</sup>

Steven A. Henck

*Texas Instruments Incorporated, Digital Imaging Components, PO Box 655012, MS992, Dallas, TX 75265, USA*  
E-mail: hen@msg.ti.com

Nearly fifty lubricants have been investigated for use in the Digital Micromirror Device<sup>TM</sup> (DMD<sup>TM</sup>). The exploration has ranged from self-assembled monolayers (SAMs), to fluids, to solid lubricants. This paper discusses several of the various approaches that have been taken to lubricate this microelectromechanical systems (MEMS) device and to reduce the adhesion between its contacting surfaces.



## Perfluoroalkanoic Acids (PFDA)

- Perfluorinated n-alkanoic acids, are deposited on the DMD by a **vapor condensation** method
- The films provide a very low-energy surface
- However, the films are **vulnerable** to ionic or solvent chemical attacks
- **Moisture** can break the bond to the surface and solvate the PFDA, thus removing it from the surface
- In addition, **thermal desorption** can occur at temperatures within the desired operating range of the device

## Perfluoroalkanoic Acids (PFDA)

- This can be an **advantage** since it is believed that vapor-phase PFDA can then **re-adsorb** to sites deficient in PFDA
- To ensure robust, reliable operation, a **hermetic chip package** must be used, which keeps the **moisture** out and an **over-pressure** of PFDA in
- Encapsulated in this fashion, the DMD lubricated with PFDA has proved to be a reliable product capable of **running at high duty cycles for many years**
- In accelerated life testing, devices have been operated for the equivalent lifetime of **20 years**

# Wafer Level Anti-Stiction Coatings for MEMS<sup>07</sup>

R. Maboudiana's Group, U.C. Berkeley  
Sensors and Actuators A, 2003

## Abstract

This paper describes a processing method which allows for the application of a **dichlorodimethylsilane (DDMS)** anti-stiction **monolayer** to MEMS devices on a wafer scale from the **vapor** phase. By utilizing vapor phase processing, many problems associated with liquid processing can be overcome. We have designed and built a **reactor** system that allows for the vapor phase deposition of a variety of anti-stiction coatings on both **die** and full 200 mm **wafer** levels. Contact angle analysis, atomic force microscopy (AFM) and thermal annealing have been used to characterize the film on Si(100). Film properties such as apparent work of adhesion and coefficient of static friction are obtained from coated micro-machine test structures. It is shown that the DDMS mono-layer deposited from the vapor phase is **as effective** at **reducing adhesion and friction** as the DDMS monolayer deposited from the (conventional) liquid phase. Moreover, it is shown that the DDMS coating can be successfully applied to a 150 mm wafer of **released devices**. Post-packaging data show substantial improvement in the stiction behavior of coated devices versus uncoated devices.

# Introduction

- Develop a **dry** process which allows for the deposition of an anti-stiction **monolayer** at the **wafer level**
- The monolayer must **survive** other post-processing steps, such as packaging, **but not impede** such processes
- The coating process must be one that can easily be adapted to industrial settings, have the potential for automatic control, and satisfy uniformity constraints
- The DDMS precursor deposited from vapor phase and a process around these constraints

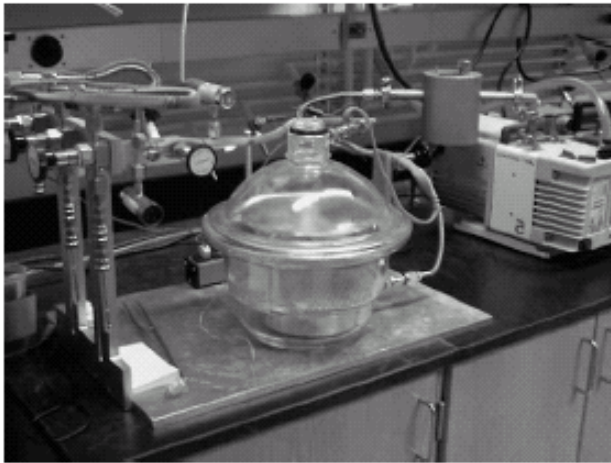
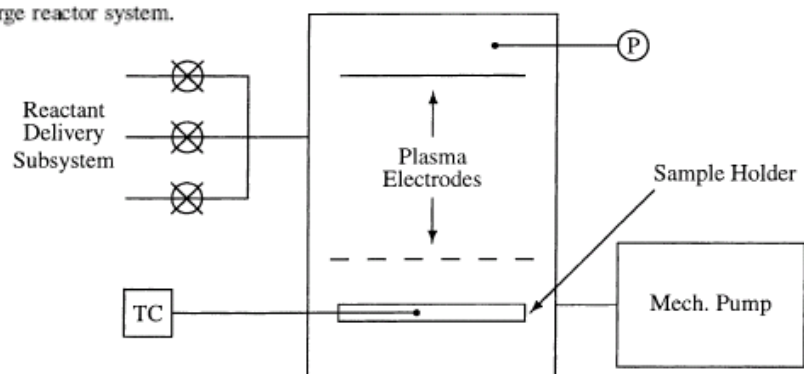


Fig. 3. A photograph of the large reactor system.



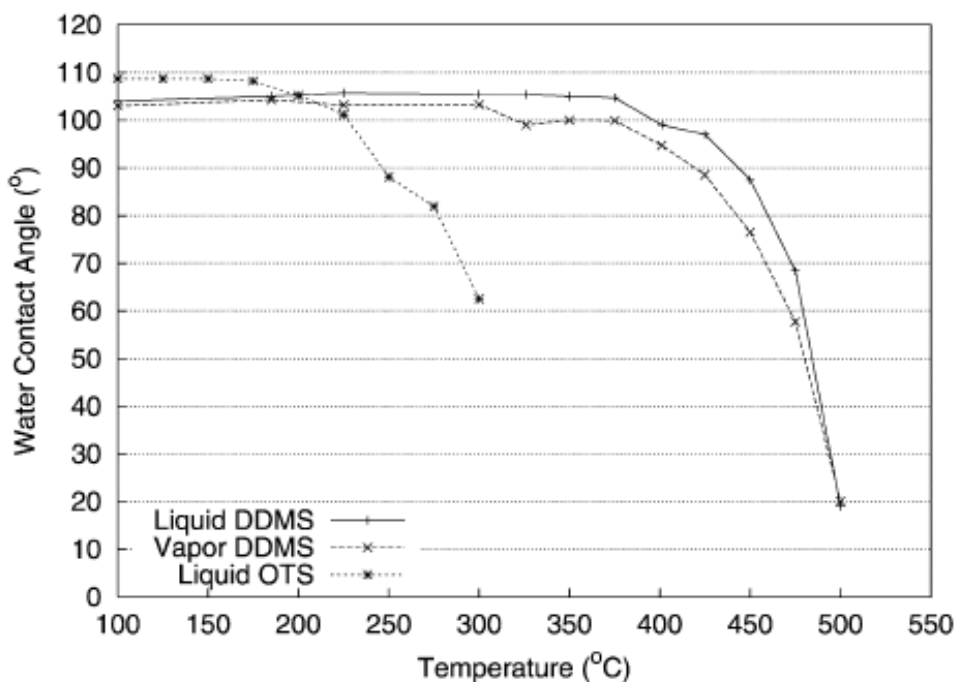
# Comparison

Selected properties of the DDMS monolayer deposited from vapor phase vs. liquid phase

Coating	$\theta_{\text{H}_2\text{O}}$ (°)	$\theta_{\text{HD}}$ (°)	$l_d$ (μm)	$\mathcal{W}$ (μJ/m <sup>2</sup> )	$\mu_s$
DDMS vapor	102	38	510	62	0.35
DDMS liquid	103	38	550	45	0.28
OTS	110	38	750	12	0.07
Oxide	0–30	0–20	< 150	20000	1.1

OTS and oxide values are given for comparison. Property data are water contact angle, hexadecane contact angle, detachment length, apparent work of adhesion, and coefficient of static friction (sidewall), respectively.

# Comparison



# Fluorocarbon Films

- The field-free zone of a plasma reactor is employed to produce a relatively conformal polymerized fluorocarbon film growth
- The FC films were found to withstand temperatures of up to 400 °C
- 20-nm-thick films can withstand  $10^8$  collapse cycles without any noticeable degradation

## Diamond-like Carbon Coating

- These films are hard, hydrophobic, exhibit relatively low surface energies, and can also be doped to enhance their electrical conductivity
- Other properties such as thermal stability, chemical inertness, and the ability to be deposited at or near room temperature make DLC an ideal candidate for integration into the micromachine fabrication process



# Tribological Impact of SiC Encapsulation of Released Poly- Crystalline Silicon Microstructures<sup>07</sup>

R. Maboudiana's Group, U.C. Berkeley  
Tribology Letters, 2004

## Abstract

A method for coating released polysilicon microstructures with thin, uniform and conformal coatings of SiC derived from the single source precursor, 1,3-disilabutane (DSB) has been developed. This coating method has been successfully applied to micro-mechanical test devices which allow evaluation of friction and wear properties of the coating. Here, data on the coefficient of static friction of SiC coatings produced from DSB is presented. Also, a comparative wear study for devices which have been oxidized, treated with an anti-adhesion coating, and SiC coated is shown. Wear is examined by scanning electron microscopy (SEM) on devices which have been cycled repetitively under a nominal load. It is found that the application of a few nanometers-thin SiC coating provides exceptional wear resistance as well as significant reduction in friction on the microscale.

# Introduction

- Although silicon is a good structural material for the microscale, owing to its **high elastic modulus and low density**, small area contacts (as in contact points between two rough surfaces) can generate enormous contact pressures which can create **plastic deformations** in silicon
- For example, the hubs on micro-gears can become visibly cluttered with **wear debris** after a few hundred thousand cycles
- These micro-gears seldom last more than a few million cycles before the build-up of wear debris and increased **friction** irreversibly bind the gear

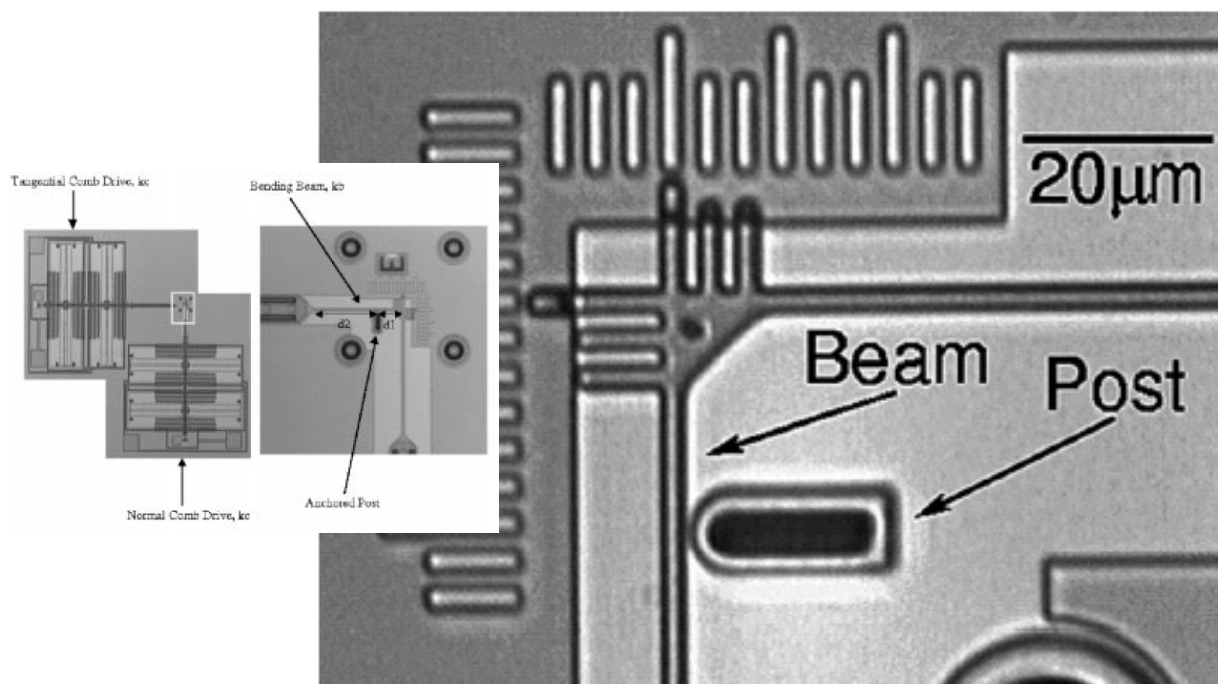
## Silicon Carbide

- An attractive material for demanding **mechanical** and **high temperature** applications
- Exceptional **tribological** properties and **corrosion** resistance
- The most conventional method for heteroepitaxial growth of 3C-SiC on Si requires **high growth temperatures** (typically > 1000 °C)

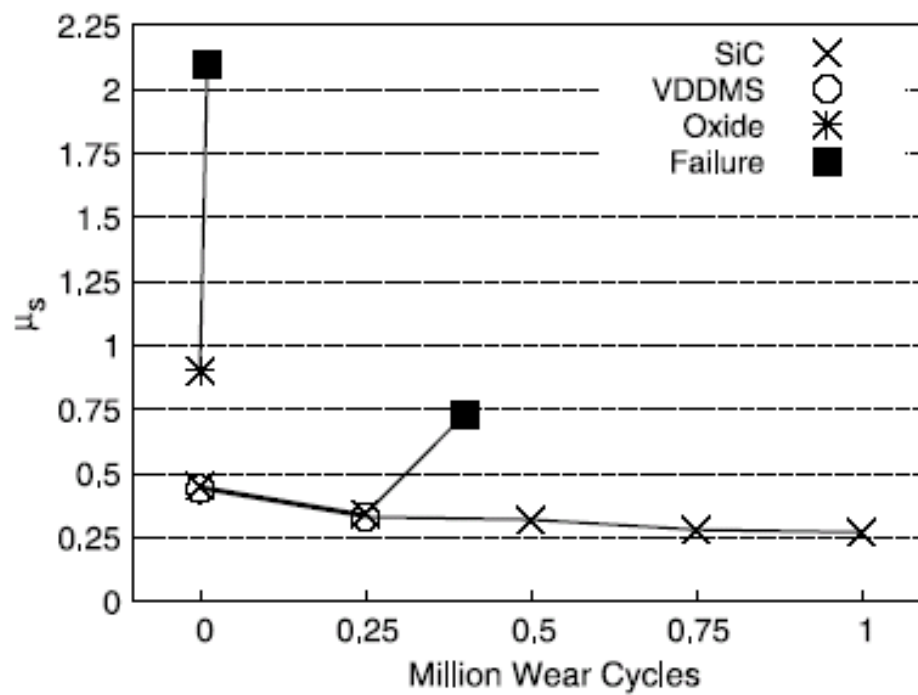
# Process Flow

- Releasing the polysilicon microdevices and coating them with an octadecene based monolayer to avoid the problem of release stiction
- The samples are introduced into the CVD chamber and heated to the deposition temperature (800 °C) at about 50 °C/min
- The DSB flow is initiated (pressure of DSB ~25 mTorr) at about 3 sccm, and maintained for an amount of time to deposit about 40~50 nm of SiC on the structures (about 5~7 min)
- The samples are then slowly cooled and removed from the CVD system

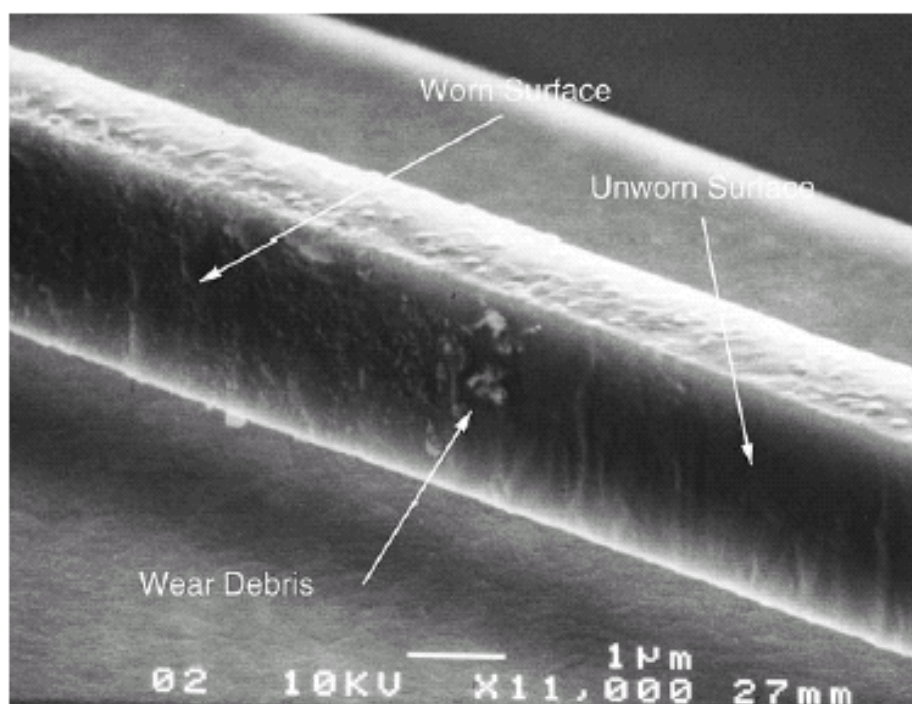
## Test Structure



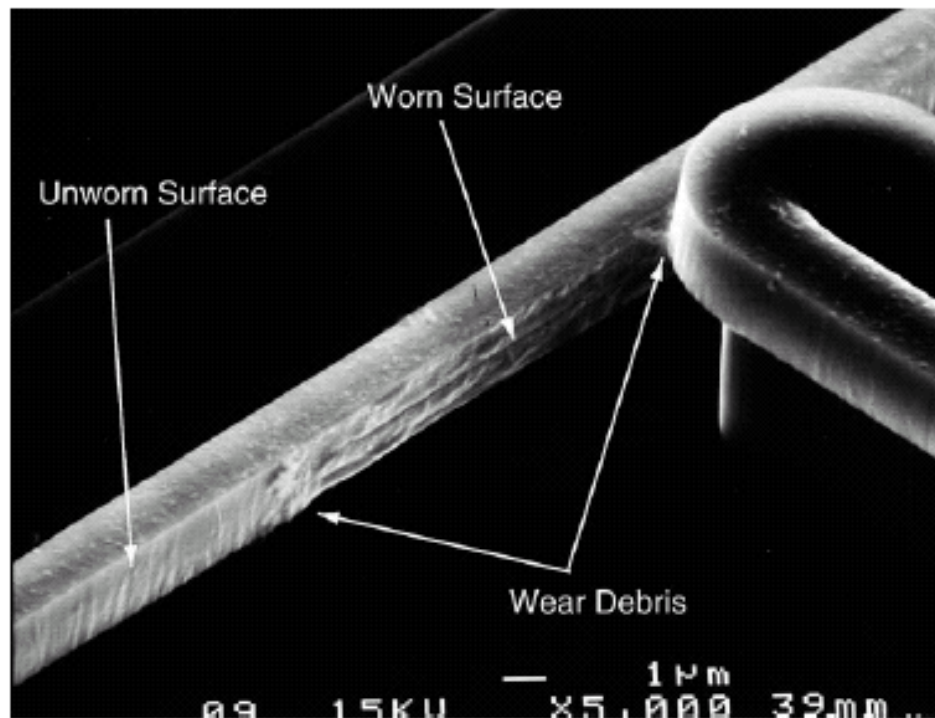
# Wear with Various Treatments



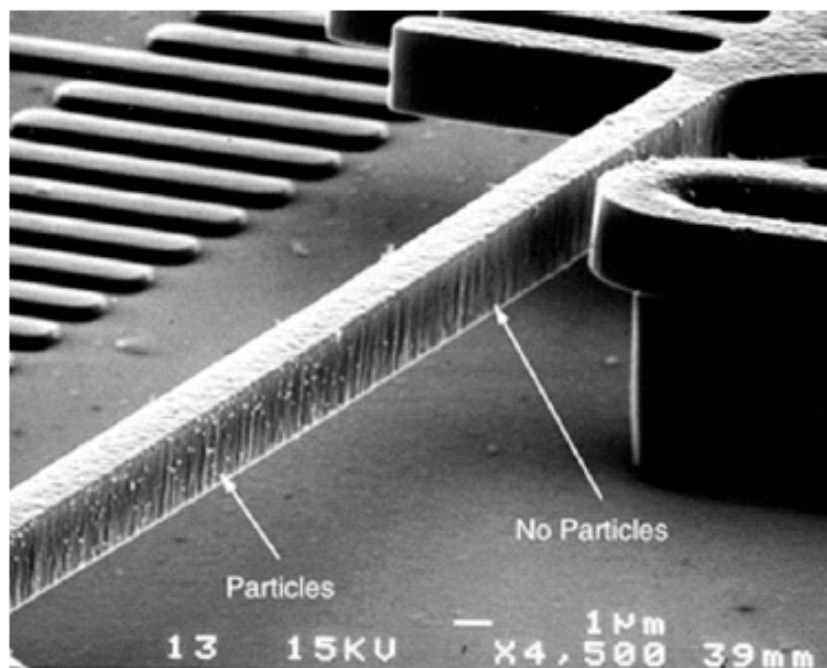
## Oxide



# VDDMS



# SiC



# Comparison

- The **oxide** surfaces were initially very clean and failed in a short amount of time, indicating that **there was no lubricating layer that could be formed at the rubbing interfaces**
- For VDDMS, there was initially a monolayer of methyl groups present at the surface. In the initial stages of wear, this source of **carbon** may lead to **the production of a lubricating layer**, which manifests itself as an apparent decrease in  $u_s$ . Over time, as more and more debris is formed, this layer may be **rubbed off** the surface, and (having **no** additional carbon to replace it)  $u_s$  increases until the device fails
- The SiC coated devices also have **carbon** available for the formation of a lubricating layer. However, the wear rate is imperceptibly low under these test conditions, and should the lubricating layer become worn, it could be renewed by consuming SiC. Thus the SiC coated devices exhibited a relatively sharp decrease in  $u_s$  as the lubricating layer is formed, and as the wear cycles accumulate, the layer persists, which is manifested as a stable value for  $u_s$ .